

within about 0.018 cm. Some difficulty is encountered with specimens which barrel excessively by slipping on two sets of orthogonal slip planes or which distort by slipping on oblique {110} slip planes. This is easily noted by the appearance of the crystal after deformation;  $\tau$ - $\epsilon$  curves in these cases show excessive work hardening rates and are omitted from these results.

In the work of Aladag *et al.* (1970) (ADG) on NaCl a variation of  $d\tau_{III}/dP$  (at  $\dot{\epsilon} \simeq 5 \times 10^{-4}/\text{sec}$ ) for different sets of crystals was noted. It is necessary, therefore, to establish the pressure behaviour of the  $\tau$ - $\epsilon$  curves at the low strain rate for the present material in order to be certain of a valid comparison with new data at the high strain rate. We note also that here  $\tau_{III}$  is defined, following Hesse (1965), as the stress at which the  $\tau$ - $\epsilon$  curve deviates by 1% (in  $\tau$ ) from the linear extrapolation of stage II. ADG employed the technique discussed by Haasen (1958) where the intersection of straight lines drawn through stages II and III is denoted as  $\tau_{III}$ . The latter technique appears less certain and is abandoned here.

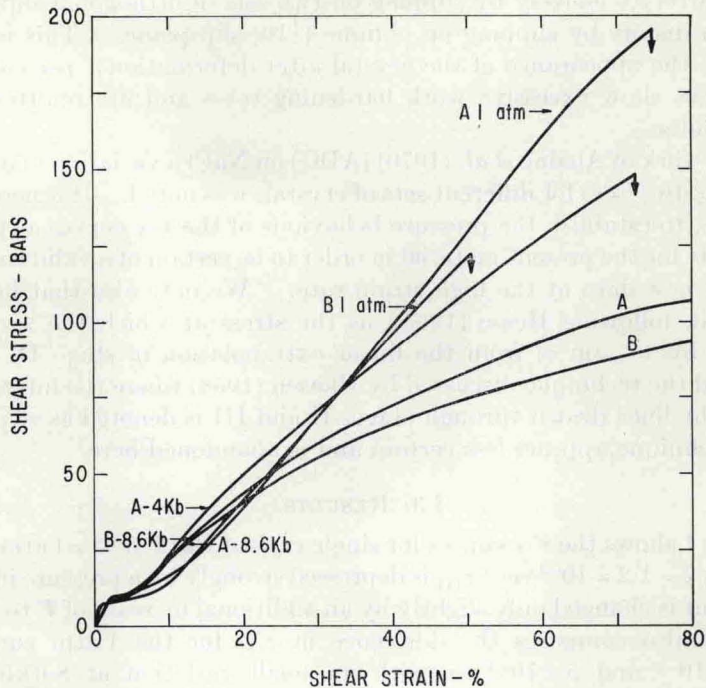
### § 3. RESULTS

Figure 1 shows the  $\tau$ - $\epsilon$  curves for single crystal NaCl at  $P = 1$  atm, 4 and 8.6 kb for  $\dot{\epsilon} = 1.2 \times 10^{-2}/\text{sec}$ ;  $\tau_{III}$  is depressed strongly by a pressure increase of 4 kb but is changed only slightly by an additional increase of  $P$  to 8.6 kb. Figure 1 also compares the difference in  $\tau_{III}$  for the 1 atm curves at  $\dot{\epsilon} = 1.2 \times 10^{-2}$  and  $5 \times 10^{-4}/\text{sec}$  with its small variation at 8.6 kb. For these curves  $\tau_s = \tau_c/2$  and  $\epsilon_s = 4\epsilon_c$ , where s and c refer to shear and compression.

Considering the data in more detail, it is found that  $\tau_I$ , the extrapolated critical resolved shear stress, is independent of  $P$  and  $\dot{\epsilon}$  within experimental scatter; at  $\dot{\epsilon} = 5 \times 10^{-4}/\text{sec}$ ,  $\tau_I = 8.0 \pm 1.2$  bars and at  $\dot{\epsilon} = 1.2 \times 10^{-2}/\text{sec}$ ,  $\tau_I = 8.7 \pm 1.4$  bars for the range 0–10 kb, where the limits represent the standard deviation. (In order to obtain an accurate estimate of the pressure dependence of  $\tau$  in stage I it is necessary to perform pressure cycling tests (Davis and Gordon 1968).) At the low strain rate, the stress for initiation of stage II,  $\tau_{II}$ , is roughly independent of pressure ( $\tau_{II} = 12.4 \pm 1.7$  bars); at  $\dot{\epsilon} = 1.2 \times 10^{-2}/\text{sec}$ ,  $\tau_{II}$  averages  $13 \pm 1.8$  bars at 2 kb and above but appears to be slightly greater at 1 atm ( $16.6 \pm 2.1$  bars) where the transition from stage I to stage II is very gradual.

The scatter in the data for  $\theta_I$  and  $\theta_{II}$ , the slopes of stages I and II, respectively, is quite considerable, but in each case trends are apparent which may be characterized by a least squares, straight line fit. For  $\dot{\epsilon} = 5 \times 10^{-4}/\text{sec}$   $\theta_I = 1.36P + 71$  (19) and  $\theta_{II} = -10P + 306$  (32), while at  $\dot{\epsilon} = 1.2 \times 10^{-2}/\text{sec}$ ,  $\theta_I = 3.2P + 76$  (20) and  $\theta_{II} = -9.4P + 316$  (54), where  $\theta$  is given in bars/unit shear strain when  $P$  is in kilobars; numbers in parentheses are the square root of the error mean square for each equation and indicate the magnitude of the scatter of the data points about the fitted straight line. At high pressure, then,  $\theta_I$  increases slightly, while  $\theta_{II}$  decreases by about  $\frac{1}{3}$  between 0 and 10 kb.

Fig. 1



$\tau$ - $\epsilon$  curves for 1 atm, 4 and 8.6 kb for  $\dot{\epsilon} = 1.2 \times 10^{-2} \text{ sec}^{-1}$  (marked A) and 1 atm and 8.6 kb for  $\dot{\epsilon} = 5 \times 10^{-4} \text{ sec}^{-1}$  (marked B); position of horizontal arrows indicates  $\tau_{III}$ . Curves at 1 atm and 4 kb terminated by fracture, those at 8.6 kb did not. The strain to fracture at 1 atm scatters over a considerable range independent of  $\dot{\epsilon}$ . Curves at 8.6 kb are typical also of those run at 6.9 and 10 kb.

Figures 2, 3 and 4 indicate the dependence on  $P$  and  $\dot{\epsilon}$  of  $\tau_{III}$ , or the stress for initiation of stage III, ( $\epsilon_{III} - \epsilon_{II}$ ), or the range of stage II, and  $\epsilon_{II}$ , or the range of stage I, respectively. In each case it is noted that the stress or strain variable decreases with  $P$ , the decrease being more rapid at the higher strain rate. A least squares analysis of the data between 1 atm and 4 kb of figs. 2 and 3 yields

$$(\partial \ln \tau_{III} / \partial P) \simeq -0.34/\text{kb}$$

and

$$(\partial \ln (\epsilon_{III} - \epsilon_{II}) / \partial P) \simeq -0.31/\text{kb}$$

for

$$\dot{\epsilon} = 1.2 \times 10^{-2} / \text{sec}$$

and

$$(\partial \ln \tau_{III} / \partial P) \simeq -0.25/\text{kb}$$

and

$$(\partial \ln (\epsilon_{III} - \epsilon_{II}) / \partial P) \simeq -0.26/\text{kb}$$

for

$$\dot{\epsilon} = 5 \times 10^{-4} / \text{sec}.$$